J. W. HUTCHINSON
Professor,
Division of Engineering
and Applied Physics,
Harvard University,
Cambridge, Mass.

On the Postbuckling Behavior of Imperfection-Sensitive Structures in the Plastic Range[1]

Aspects of postbuckling behavior are investigated for structures undergoing plastic deformation. The structures singled out are characterized by a highly imperfection-sensitive behavior where buckling takes place in the elastic range. A simple model study is carried out and is followed by an analysis of the plastic buckling of a complete spherical shell under external pressure. In both instances, the bifurcation behavior and subsequent deformation of the perfect structure as well as the influence which geometric imperfections have on buckling are studied.

Introduction

Elastic structures which are labeled imperfection-sensitive have the property that when a perfect realization of the structure undergoes bifurcation the load carrying capacity diminishes, and the bifurcation load is the (local) maximum load that can be supported. Small imperfections arising from various sources usually have an appreciable effect on the maximum load such a structure can support. On the other hand, when bifurcation occurs in the plastic range it is generally true that bifurcation must take place under increasing applied load. At least this is what happens according to the Shanley concept [1–4],[2] and Hill's [5, 6] general study of the bifurcation behavior of elastic-plastic solids suggests that this is the rule rather than the exception.

For an elastic system, a study of the equilibrium configurations in the neighborhood of the bifurcation point reveals its stability characteristics. If the structure is imperfection-sensitive and if small imperfections are accounted for in the analysis, then exact asymptotic results relating the buckling load (local maximum) to the imperfection amplitude can be obtained [7–9]. An analysis of the plastic buckling of imperfection-sensitive structures, similar in spirit to Koiter's analysis of elastic systems, has not been accomplished in part, no doubt, due to the considerable complications which accompany the introduction of elastic-plastic behavior. In fact, it seems unlikely that results as general and concise as those for elastic systems will be obtainable.

In this paper we focus on the postbuckling behavior of structures which are imperfection-sensitive when buckling takes place in the elastic range. First, a simple model study is carried out which does yield some simple and revealing formulas for the effect of small imperfections. The model study is followed by an analysis of the plastic buckling of a complete spherical shell. A brief review of the bifurcation behavior of the perfect sphere is given, and a numerical analysis of the axisymmetric postbuckling deformation of perfect and imperfect spherical shells is reported.

Buckling of an Imperfection-Sensitive Simple Model in the Plastic Range

Significant imperfection-sensitivity of elastic structures is due to strong geometric, or structural, nonlinearities. These nonlinearities will be equally important when buckling takes place in the plastic range. The simple model investigated here combines the essential features of Shanley's [1] model of plastic column buckling and Karman, Dunn, and Tsien's [10] model of elastic buckling of imperfection-sensitive structures. It is similar in a number of respects to models studied by Sewell [11] and Augusti [12] but differs in that the model possesses a strong geometric nonlinearity and this property is exploited in the analysis. An elastic version of the model was used to study dynamic buckling in reference [13].

[1] This work was supported in part by the National Aeronautics and Space Administration under Grant NGL 22-007-012, and by the Division of Engineering and Applied Physics, Harvard University.

[2] Numbers in brackets designate References at end of paper.

Contributed by the Applied Mechanics Division for publication (without presentation) in the Journal of Applied Mechanics. Discussion on this paper should be addressed to the Editorial Department, ASME, United Engineering Center, 345 East 47th Street, New York, N. Y. 10017, and will be accepted until April 20, 1972. Discussion received after the closing date will be returned. Manuscript received by ASME Applied Mechanics Division, August 14, 1970; final revision, December 4, 1970. Paper No. 71-APM-FF.

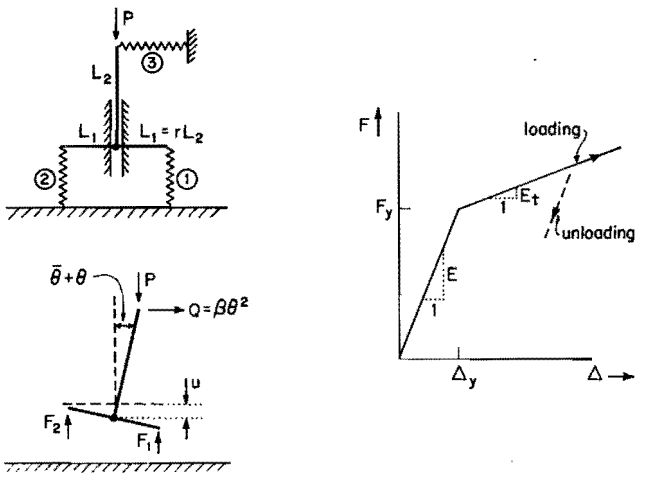

Fig. 1 Simple model and load-deflection relation for springs Nos. 1 and 2

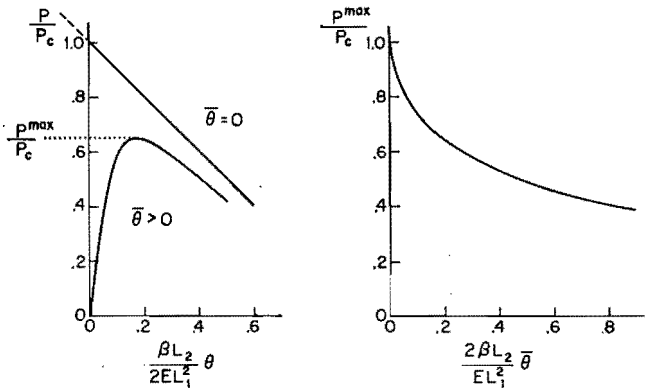

Fig. 2 Buckling behavior of model in elastic range

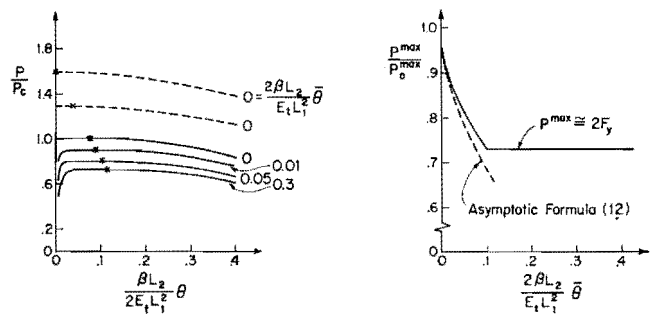

Fig. 3 Buckling behavior of model in plastic range with $E_t/E = 0.25$, $\beta/(E_tL_1) = 10$ and $\Delta_yL_2/L_1^2 = 0.18$ (asterisk denotes maximum load $P_c = 2E_trL_1$ and P_0^{max} is the maximum load for $\bar{\theta} \to 0$)

The rigid-rod model, which is shown in Fig. 1, can displace vertically as measured by u and can rotate as measured by θ. An initial rotation from the vertical in the unload state is called the imperfection and is denoted by $\bar{\theta}$ so that the total rotation is $\bar{\theta} + \theta$. The load-deflection behavior of each of the supporting springs, Nos. 1 and 2, is also shown in Fig. 1 and is given by

$$\dot{F} = E\dot{\Delta} \text{ for } \begin{cases} F < F^{max}, \text{ or} \\ F = F^{max} \text{ and } \dot{F} < 0 \end{cases} \quad (1)$$

$$\dot{F} = E_t\dot{\Delta} \text{ for } F = F^{max} \text{ and } \dot{F} > 0$$

where $F^{max} = F_y$ for initial yield. Spring No. 3 is introduced to bring in a strong geometric nonlinearity. Under a rotation θ the force which develops in this spring is $Q = \beta\theta^2$. We shall assume that the parameter $\beta/(EL_1)$ is large compared to unity. This insures that Q is the only significant geometric nonlinearity and permits us to replace sin θ and cos θ by θ and 1, respectively.

The equations of equilibrium and the deflection-displacement relations are

$$F_1 + F_2 = P \quad (2)$$

$$(F_2 - F_1)L_1 + PL_2(\bar{\theta} + \theta) + \beta L_2\theta^2 = 0 \quad (3)$$

$$\Delta_1 = u + L_1\theta$$
$$\Delta_2 = u - L_1\theta \quad (4)$$

where the subscripts denote springs Nos. 1 and 2.

The behavior of the model for a purely elastic response ($E_t = E$) is shown in Fig. 2. Bifurcation of the perfect structure occurs at $P_C = 2ErL_1$; and the maximum support load in the presence of an imperfection, $\bar{\theta} > 0$, is given by

$$\left(1 - \frac{P^{max}}{P_C}\right)^2 = \left(\frac{2\beta}{ErL_1}\bar{\theta}\right)\frac{P^{max}}{P_C} \quad (5)$$

For $\bar{\theta}$ sufficiently small,

$$\frac{P^{max}}{P_C} = 1 - \left(\frac{2\beta}{ErL_1}\bar{\theta}\right)^{1/2} + \ldots \quad (6)$$

Turning to plastic buckling, we first consider the bifurcation behavior of the model with no imperfection. The lowest value of P at which bifurcation is possible is $P^{tan} = 2E_trL_1$, the so-called tangent modulus load; but bifurcation is possible for any $P \geq P^{tan}$. The interesting case is when $\theta \geq 0$ for which spring No. 1 continues to load and spring No. 2 unloads coincident with bifurcation. If bifurcation occurs at $P = P_C$ then the load-deflection relation is

$$P = \left[P_C + \frac{1}{r}\left(\frac{1+\lambda}{1-\lambda}\right)P^{rm}\theta - \frac{\beta}{r}\left(\frac{1+\lambda}{1-\lambda}\right)\theta^2\right] \times \left[1 + \frac{1}{r}\left(\frac{1+\lambda}{1-\lambda}\right)\theta\right]^{-1} \quad (7)$$

$$\cong P_C + \theta\left[\frac{1}{r}\left(\frac{1+\lambda}{1-\lambda}\right)(P^{rm} - P_C)\right] - \theta^2\left[\frac{1}{r^2}\left(\frac{1+\lambda}{1-\lambda}\right)^2(P^{rm} - P_C) + \frac{\beta}{r}\left(\frac{1+\lambda}{1-\lambda}\right)\right] + \ldots \quad (8)$$

where $\lambda = E_t/E$. The reduced modulus load where bifurcation takes place with no change in the applied load, to first order, is given by

$$P^{rm} = \frac{2P^{tan}}{1+\lambda}$$

For $P_C < P^{rm}$, bifurcation takes place under increasing load. The maximum load which the perfect structure can support when bifurcation occurs at $P_C = P^{tan}$ satisfies the equation

$$(P^{rm} - P_0^{max})^2 + 4\beta r\left(\frac{1-\lambda}{1+\lambda}\right)(P^{tan} - P_0^{max}) = 0 \quad (9)$$

or

$$P_0^{max} = P^{tan}\left[1 + \frac{E_tL_1}{2\beta}\left(\frac{1-\lambda}{1+\lambda}\right) + \ldots\right]$$

This value is only very slightly above the bifurcation load.

An example of the load-deflection relation (7) is plotted in Fig. 3 for three different bifurcation values. In this figure P is normalized by $P_C = P^{tan}$ and this curve is shown as a solid line ($\bar{\theta} = 0$). The upper dashed curve corresponds to bifurcation

at the reduced modulus load, while bifurcation takes place halfway between P^{rm} and P^{tan} for the lower dashed curve. On each curve, the maximum load occurs at the point marked by a cross. Our discussion this far follows that given in more detail by Sewell [11] for a similar model.

In the presence of a small imperfection, $\bar{\theta} > 0$, the load-deflection behavior is considerably more complicated. There are three distinct sequences of loading and unloading which can take place depending on the magnitude of $\bar{\theta}$. First, consider the case for which $\bar{\theta}$ is sufficiently small so that the resulting formulas will be valid in the limit as $\bar{\theta}$ vanishes. In this case, it is found that there are four separate steps to the loading history. With the first application of load both springs are elastic. Next, spring No. 1 starts deforming plastically and is followed by spring No. 2 at a slightly higher load. The load continues to rise. At a value of θ, denoted by $\hat{\theta}$, spring No. 2 unloads. From this point on spring No. 1 loads while No. 2 stays in the elastic range.

The maximum value of P occurs at a value of θ slightly larger than $\hat{\theta}$. Some of the formulas for the values of P and θ at the various stages of the history are rather lengthy and will not be listed here.[3] On the other hand, the expressions for $\hat{\theta}$ and P^{max} are relatively simple. They are independent of F_y and are given by

$$\hat{\theta} = -\bar{\theta} + \left\{\bar{\theta}^2 + \frac{r\bar{\theta} - \bar{\theta}^2}{1 + \beta/(2E_tL_1)}\right\}^{1/2} \tag{10}$$

and

$$P^{max} = P_0^{max} - 2\beta\left[\hat{\theta} + \left\{\left(1 + \frac{2E_tL_1}{\beta}\right)^{1/2} - 1\right\}(\hat{\theta} + \bar{\theta})\right] \tag{11}$$

Asymptotically for small $\bar{\theta}$, equation (11) becomes

$$\frac{P^{max}}{P_0^{max}} = 1 - \left(\frac{2\beta}{E_trL_1}\bar{\theta}\right)^{1/2} + \ldots \tag{12}$$

where it is recalled that P_0^{max} is the maximum support load (9) of the perfect structure when bifurcation occurs at $P_C = P^{tan}$.

The asymptotic result (12) is particularly expressive in that it is very similar to the analogous result (6) for the purely elastic model. The important difference is the presence of E_t in (12) rather than E. Thus, for small imperfections, the model is more imperfection-sensitive in the plastic range than in the elastic range in the sense that an imperfection amplitude $\lambda\bar{\theta}$ results in the same relative reduction of the buckling load as does $\bar{\theta}$ in the elastic case.

Equation (11) ceases to hold when $\bar{\theta}$ is sufficiently large such that spring No. 2 does not become plastic at all. In this sequence of loading, spring No. 1 yields at a value of P just under $2F_y$ and the model deflects readily under only slightly increasing load until the maximum load occurs at a value which is given very closely by

$$P^{max} \cong 2F_y \tag{13}$$

Curves of P versus θ for the example in Fig. 3 are also shown for nonzero values of $\bar{\theta}$. The parameters of the model have been chosen such that P^{tan} (P_C in Fig. 3) is 40 percent higher than $2F_y$, the initial yield value for the perfect model. Curves of the maximum load as a function of the imperfection $\bar{\theta}$ are shown on the right in Fig. 3. The asymptotic prediction (12) is shown as a dashed curve and agrees very closely with the exact result until second branch (13) governs.

If the "elastic buckling load," $2ErL_1$, is only slightly higher than the plastic value, $2E_trL_1$, a third possibility arises in which

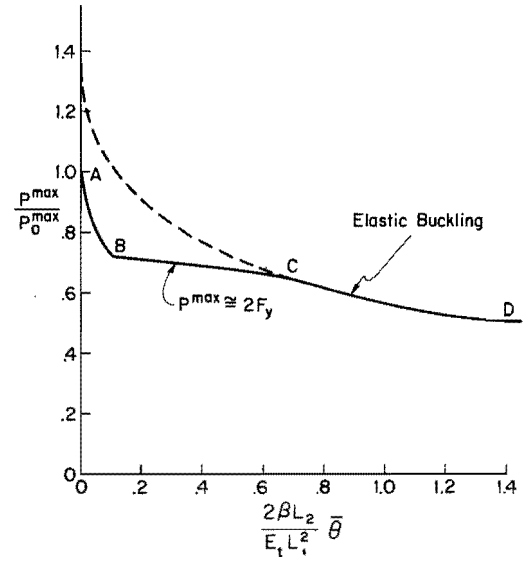

Fig. 4 Buckling of model for a case in which the plastic buckling load of the perfect model is only slightly below the elastic buckling load ($E_t/E = 0.75$, $\beta/(E_tL_1) = 10$, and $\Delta_y L_2/L_1^2 = 0.525$)

for sufficiently large imperfections neither spring becomes plastic before the maximum load occurs. On this branch (5) holds. Thus, for example, if a structure is highly imperfection-sensitive an imperfection of modest size may trigger buckling before any plastic deformation sets in even though the perfect structure would buckle in the plastic range.[4] The example shown in Fig. 4 illustrates this behavior. Here $E_t/E = 3/4$ so that the elastic buckling load is only one-third greater than the tangent modulus load. Branch A-B displays the strong imperfection-sensitivity associated with equation (11), while on B-C (13) holds. On C-D the maximum load is attained before any plastic deformation takes place as discussed.

Bifurcation Behavior of a Perfect Spherical Shell in the Plastic Range

The critical external pressure for *elastic* buckling of a perfect complete spherical shell is

$$p_C = \frac{2E}{[3(1 - \nu^2)]^{1/2}}\left(\frac{t}{R}\right)^2 \tag{14}$$

where t is the shell thickness, R is its radius, and the isotropic elastic properties are specified by the Young's modulus E and Poisson's ratio ν. The principle in-plane stresses are equal and are given by $\sigma_C = -p_CR/(2t)$. Associated with this critical pressure is a multiplicity of $(2n + 1)$ linearly independent buckling modes whose displacements normal to the shell middle surface are given in terms of the spherical surface harmonics of degree n:

$$w = S_n(\theta, \phi) = a_0P_n(\cos\theta) + \sum_{m=1}^{n} P_n^{(m)}(\cos\theta) \times [a_m \cos m\phi + b_m \sin m\phi] \tag{15}$$

where θ is the polar angle and ϕ is the longitudinal coordinate. The degree n is the integer which most closely satisfies

[3] I am indebted to N. L. Goldman for a careful check of the analysis of the simple model.

[4] Some specific calculations for cylindrical shells under axial compression suggest that the opposite can be true [14]; namely, that an imperfection may induce high local stresses and plastic deformation (which tend to reduce the buckling load) even though the perfect shell would buckle in the elastic range.

$$n(n+1) = 2[3(1-\nu^2)]^{1/2}\frac{R}{t} \tag{16}$$

and P_n is the Legendre polynomial of degree n and $P_n^{(m)}$ is the associated polynomial of degree n and order m.

This result in its general form is due to van der Neut [15]. We have taken the previous formulas from a recent paper by Koiter [16] who has rederived these results using the simpler Donnell-Mushtari-Vlasov shell equations which are entirely adequate for this problem due to the shallow character of the buckling deformations.

The state of stress in a perfect spherical shell prior to bifurcation is a purely membrane one with equal principle in-plane stresses whether or not the shell has undergone plastic deformation. Thus the relationship between the in-plane stress rates and strain rates at bifurcation is necessarily isotropic for any plasticity theory with a single plastic branch as long as no elastic unloading occurs. Therefore, it is possible to introduce an effective tensile modulus E_e and Poisson's ratio ν_e relating in-plane stress and strain rate quantities. Under the usual assumptions for thin shells that the Kirchhoff-Love hypotheses apply, the lowest bifurcation pressure in the plastic range is still given by (14) but with E replaced by E_e and ν by ν_e; i.e.,

$$p_C = \frac{2E_e}{C_e}\left(\frac{t}{R}\right)^2 \tag{14a}$$

where $C_e = [3(1-\nu_e^2)]^{1/2}$. The same axisymmetric and nonaxisymmetric bifurcation modes (15) are possible (coupled with a uniform radial displacement rate) if ν is replaced by ν_e in (16). Bijlaard [17] was apparently the first to note that (14), appropriately modified, holds in the plastic range. It is rigorously valid within the context of first-order shell theory as long as the bifurcation modes are sufficiently shallow, that is, as long as n given by (16) is sufficiently large ($n \geq 6$ or 7 is probably a reasonable cutoff.

Bifurcation at the value p_C given by (14a) is only possible if no elastic unloading occurs anywhere in the shell [1, 5]. The rate of change of the J_2 stress invariant at the bifurcation point with loading everywhere can be obtained by a straightforward analysis which employs the bifurcation rate of the normal displacement (15) and the associated Airy stress function rate of Donnell-Mushtari-Vlasov shell theory. The details of this calculation are not given here. Consistent with the assumptions of thin shell theory, the J_2 invariant is taken to depend only on the in-plane stresses so that with $s_{ij} = \sigma_{ij} - \frac{1}{3}\sigma_{kk}\delta_{ij}$,

$$J_2 \equiv \tfrac{1}{2}s_{ij}s_{ij} \cong \tfrac{1}{3}(\sigma_{11}^2 + \sigma_{22}^2 + 3\sigma_{12}^2 - \sigma_{11}\sigma_{22}) \tag{17}$$

We find that at a distance z measured outward from the middle surface of the shell $\dot{J}_2$ is given by

$$\dot{J}_2 = -\frac{1}{6}\left(p_C\frac{R}{t}\right)^2\left\{C_e\left[\frac{1}{2}+\left(\frac{z}{t}\right)\frac{C_e}{1-\nu_e}\right]\frac{\dot{S}_n}{t} - \frac{\dot{p}}{p_C}\right\} \tag{18}$$

where $\dot{p}$ is the pressure rate and $\dot{S}_n$ is the bifurcation mode rate given by (15).[5] For any plasticity theory based on the J_2 invariant alone, such as simple flow theory and deformation theory discussed later, the loading condition requires $\dot{J}_2 \geq 0$ everywhere in the shell. If the buckling amplitude rate at bifurcation is denoted by $\dot{\delta}$ (i.e., $\dot{\delta} = \max[\dot{S}_n]$), then no unloading occurs as long as

$$\frac{\dot{p}}{p_C} \geq \frac{C_e}{2}\left(1+\frac{C_e}{1-\nu_e}\right)\frac{\dot{\delta}}{t} \tag{19}$$

[5] One of the reviewers has expressed the wish that the use of the terminology "rates" in static incremental plasticity would disappear from the literature and be solely reserved for time-dependent plasticity. While the economy in both language and notation does make the "rate terminology" attractive, we basically agree with his point of view and therefore use this footnote as an advertisement for this cause and as a warning that in this paper we are dealing entirely with time-independent problems.

For J_2 flow theory, for example, the effective Young's modulus and Poisson's ratio for the perfect sphere in the prebifurcation state are given by

$$\frac{1}{E_e} = \frac{1}{E}\left[1+\frac{1}{4}\left(\frac{E}{E_t}-1\right)\right] \quad \text{and} \quad \frac{\nu_e}{E_e} = \frac{1}{E}\left[\nu - \frac{1}{4}\left(\frac{E}{E_t}-1\right)\right] \tag{20}$$

where the tangent modulus E_t is a function of J_2 and is defined in the usual way by $\dot{\sigma} = E_t\dot{\epsilon}$ for a uniaxial tensile history. The critical pressure is

$$p_C = \frac{4E}{[6(1+\nu)(1-2\nu+E/E_t)]^{1/2}}\left(\frac{t}{R}\right)^2 \tag{21}$$

This formula, which was originally due to Bijlaard, was rederived by Batterman [18] under the restriction of axisymmetric deformations using equations for shells of revolution given in [19]. Batterman [18] also gives a formula similar to (19) derived specifically for J_2 flow theory and under the restriction of axially symmetric deformations.

For a J_2 deformation theory of plasticity

$$\frac{1}{E_e} = \frac{1}{4}\left(\frac{1}{E_t}+\frac{3}{E_s}\right), \quad \frac{\nu_e}{E_e} = -\frac{1}{4}\left[\frac{2(1-2\nu)}{E}+\frac{1}{E_t}-\frac{3}{E_s}\right] \tag{22}$$

and

$$p_C = \frac{4E}{\left\{3\left[3\frac{E}{E_t}\frac{E}{E_s}-(1-2\nu)\left(1-2\nu+\frac{E}{E_t}-\frac{3E}{E_s}\right)\right]\right\}^{1/2}}\times\left(\frac{t}{R}\right)^2 \tag{23}$$

where E_s is a function of J_2 and is defined in uniaxial tension to be $E_s = \sigma/\epsilon$.

Plastic Postbuckling Behavior and Imperfection-Sensitivity of a Spherical Shell Undergoing Axisymmetric Deformations

Formulation of Rate Equations and Numerical Analysis. In this section a numerical analysis of the postbuckling behavior of perfect and imperfect complete spherical shells is carried out. Our investigation is restricted to deformations and imperfections which are rotationally symmetric with respect to some axis. Interaction between the axisymmetric bifurcation mode and the many nonaxisymmetric modes (15) is likely to be important particularly if nonaxisymmetric imperfections are present; but for elastic buckling at least, there is now little doubt that the strong imperfection-sensitivity of the spherical shell is uncovered by an axisymmetric analysis [16, 20–22].

Reissner's [23] nonlinear equations for the axisymmetric deformation of shells of revolution are employed in the analysis. The strain-displacement and equilibrium equations of this shell theory are left in their uncombined form in which no dependent variable is differentiated more than once with respect to the polar coordinate θ. As discussed in more detail later, the equations governing an incremental step in the deformation history are reduced to a set of six first-order ordinary differential equations.

A small strain theory of plasticity is used in which the relation between the stress rates and strain rates for the material in the shell is assumed to be of the form

$$\dot{\sigma}_{ij} = L_{ijkl}\dot{\epsilon}_{kl} \tag{24}$$

with $L_{ijkl} = L_{jikl} = L_{ijlk} = L_{klij}$. These instantaneous moduli depend, in general, on the stress history and here it is assumed that there are two branches to $\mathbf{L}$ depending on whether loading or unloading occurs. In an approximately plane state of stress only the in-plane stresses enter into the constitutive relation and it is convenient to introduce the in-plane moduli according to

$$\dot{\sigma}_{\alpha\beta} = \hat{L}_{\alpha\beta\gamma\mu}\dot{\epsilon}_{\gamma\mu} \tag{25}$$

where the Greek indexes take on only the values 1 and 2. The in-plane moduli are related to the 3-D moduli by

$$\hat{L}_{\alpha\beta\gamma\mu} = L_{\alpha\beta\gamma\mu} - \frac{L_{\alpha\beta 33}L_{\gamma\mu 33}}{L_{3333}} \tag{26}$$

Strain-rate components a distance z outward from the shell middle surface are given in terms of the middle surface strain rates $\dot{E}_{\alpha\beta}$ and the bending strain rates $\dot{K}_{\alpha\beta}$ by

$$\dot{\epsilon}_{\alpha\beta} = \dot{E}_{\alpha\beta} + z\dot{K}_{\alpha\beta} \tag{27}$$

Using the usual definitions of the resultant stress tensor $N_{\alpha\beta}$ and the bending moment tensor $M_{\alpha\beta}$, we find

$$\dot{N}_{\alpha\beta} = H_{\alpha\beta\gamma\mu}{}^{(1)}\dot{E}_{\gamma\mu} + H_{\alpha\beta\gamma\mu}{}^{(2)}\dot{K}_{\gamma\mu} \quad \text{and} \quad \dot{M}_{\alpha\beta} = H_{\alpha\beta\gamma\mu}{}^{(2)}\dot{E}_{\gamma\mu} + H_{\alpha\beta\gamma\mu}{}^{(3)}\dot{K}_{\gamma\mu} \tag{28}$$

where

$$H_{\alpha\beta\gamma\mu}{}^{(i)} = \int_{-t/2}^{t/2} \hat{L}_{\alpha\beta\gamma\mu}z^{i-1}dz \tag{29}$$

Two phenomenological theories of plasticity will be used in the present analysis. In each of them the plastic deformation depends only on J_2 invariant (17). The instantaneous moduli for J_2 flow theory with isotropic elastic properties are

$$L_{ijkl} = \frac{E}{1+\nu}\left\{\frac{1}{2}(\delta_{ik}\delta_{jl} + \delta_{il}\delta_{jk}) + \frac{\nu}{1-2\nu}\delta_{ij}\delta_{kl} - \frac{fs_{ij}s_{kl}}{1+\nu+2fJ_2}\right\} \tag{30}$$

where for $\dot{J}_2 < 0$ or $J_2 < (J_2)_{\max}$, $f = 0$; while for $J_2 = (J_2)_{\max}$ and $\dot{J}_2 \geq 0$,

$$f = \frac{3}{4J_2}\left(\frac{E}{E_t} - 1\right) \tag{31}$$

For J_2 deformation theory (with unloading incorporated),

$$L_{ijkl} = \frac{E}{1+\nu+g}\left\{\frac{1}{2}(\delta_{ik}\delta_{jl} + \delta_{il}\delta_{jk}) + \frac{3\nu+g}{3(1-2\nu)}\delta_{ij}\delta_{kl} - \frac{g's_{ij}s_{kl}}{1+\nu+g+2g'J_2}\right\} \tag{32}$$

where

$$g' \equiv \frac{dg}{dJ_2}.$$

For unloading, $g = g' = 0$; while for loading,

$$g = \frac{3}{2}\left(\frac{E}{E_s} - 1\right) \tag{33}$$

Rate equations of equilibrium for shells of revolution undergoing axisymmetric deformations involve five stress quantities—$\dot{M}_{11}$, $\dot{M}_{22}$, $\dot{N}_{11}$, $\dot{N}_{22}$, and $\dot{Q}_1$—in the usual notation with the index 1 associated with the polar coordinate θ. The strain-rate displacement-rate equations involve four strain quantities, $\dot{E}_{11}$, $\dot{E}_{22}$, $\dot{K}_{11}$, and $\dot{K}_{22}$, two displacement rates, $\dot{u}$ and $\dot{w}$, and one rotation rate $\dot{\phi}_1$. Six of these rate quantities can be eliminated from the governing Reissner equations with the aid of the constitutive relations (28) to give a set of six first-order differential equations which in matrix notation take the form

$$\frac{d}{d\theta}\dot{\mathbf{X}} + \mathbf{A}\dot{\mathbf{X}} = \dot{\mathbf{p}} \tag{34}$$

In this equation $\dot{\mathbf{X}} \equiv (\dot{N}_{11}, \dot{Q}_1, \dot{M}_{11}, \dot{u}, \dot{w}, \dot{\phi}_1)$. The column vector $\dot{\mathbf{p}}$ depends on the loading rates and the current state of deformation of the shell through $\mathbf{X}$, and the 6×6 matrix $\mathbf{A}$ depends on the instantaneous moduli (29) and on $\mathbf{X}$. This choice of dependent variables has been used previously with success in the analysis of elastic shells of revolution [24–26] and a detailed discussion of the numerical analysis of this system of equations is given in [27].[6]

The great advantage of dealing with a system of first-order differential equations in a plasticity analysis is that no differentiation of the stiffness quantities is required. Equation (34) is cast into finite-difference form by dividing the polar coordinate, θ, into N equally spaced intervals with $N+1$ stations at which $\mathbf{X}$ is defined running from the pole to the equator. Equation (34) is replaced by

$$\frac{\dot{\mathbf{X}}_{i+1} - \dot{\mathbf{X}}_i}{\Delta\theta} + \mathbf{A}_i\left(\frac{\dot{\mathbf{X}}_{i+1} + \dot{\mathbf{X}}_i}{2}\right) = \dot{\mathbf{p}}_i \tag{35}$$

where $\mathbf{A}_i$ and $\mathbf{p}_i$ are evaluated halfway between the ith and the $i+1$th station. As discussed in [27], the boundary conditions at the pole are $Q_1 = u = \phi_1 = 0$ and these same conditions hold at the equator if the deformation is symmetric with respect to the equator.

At any stage in the loading history, instantaneous bending and stretching stiffnesses (29) are calculated by integrating the "local" moduli $\hat{L}_{\alpha\beta\gamma\mu}$ through the shell thickness. This can be accomplished in a number of ways. Here, the distance through the thickness is divided into M equal intervals and the local moduli are taken to be constant within each interval. As the deformation proceeds the stresses and $(J_2)_{\max}$ are calculated (and stored) at the midpoint of each of these intervals using (25), (27), (30), or (32). In this way, the $\hat{L}_{\alpha\beta\gamma\mu}$ are known in the M intervals through the thickness. So, for example,

$$H_{\alpha\beta\gamma\mu}{}^{(3)} = \sum_{j=1}^{M}\frac{t}{M}\left[z_j{}^2 + \frac{1}{12}\left(\frac{t}{M}\right)^2\right]\hat{L}_{\alpha\beta\gamma\mu}{}^{(j)} \tag{36}$$

where z_j is the midpoint of the jth interval.

To evaluate (36) at a particular stage of the deformation history it is necessary to anticipate whether the elastic branch or the plastic branch of each $\hat{L}_{\alpha\beta\gamma\mu}{}^{(i)}$ will be active. Of course, if $J_2 < (J_2)_{\max}$ the elastic branch is active; but if $J_2 = (J_2)_{\max}$, the actual branch depends on the stress rates from the solution to (35). A correct solution for any increment of the deformation history requires an iterative procedure to finally obtain the branches which are everywhere consistent with the sign of $\dot{J}_2$ which does occur. If the history is sufficiently smooth so that the transition from loading to unloading, or vice versa, at any point of the shell occurs only once or twice, a more straightforward approach is possible which eliminates the iterations at each step. If $J_2 = (J_2)_{\max}$ at any stage of the history, then the plastic branch is taken to be active. If $\dot{J}_2$ turns out to be negative, elastic unloading will occur in the next increment of the history. This procedure will only be accurate if the incremental steps making up an entire history are very small; but anyway, this is consistent with the necessity of taking small increments to approximate nonlinear behavior by a series of piecewise linear steps. The simpler procedure was used in calculating the results reported here. An indication of the accuracy of the method and the number of stations required, both through the thickness and along the longitude, is discussed in conjunction with the numerical results.

Numerical Results. A Ramberg-Osgood-type relation between

[6] A Potters-type routine for the solution of the banded matrix which arises when the equations are finite-differenced was kindly supplied by W. B. Stephens.

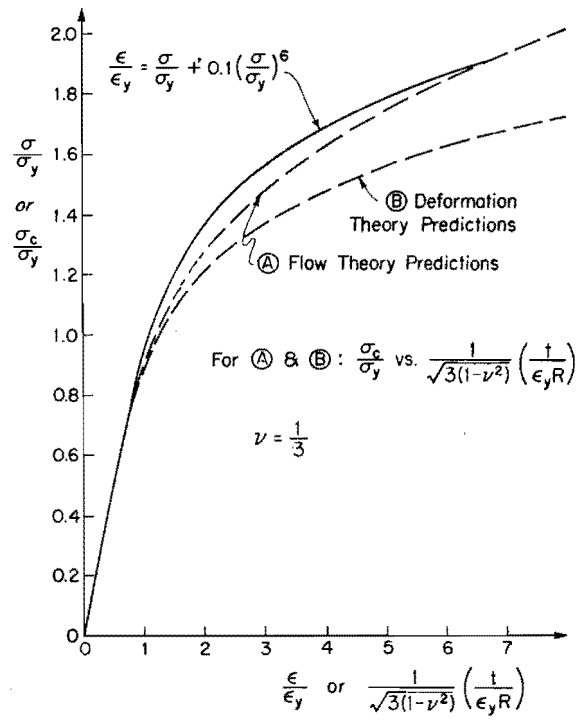

Fig. 5 Tensile stress-strain curve and bifurcation stresses for a perfect spherical shell under external pressure

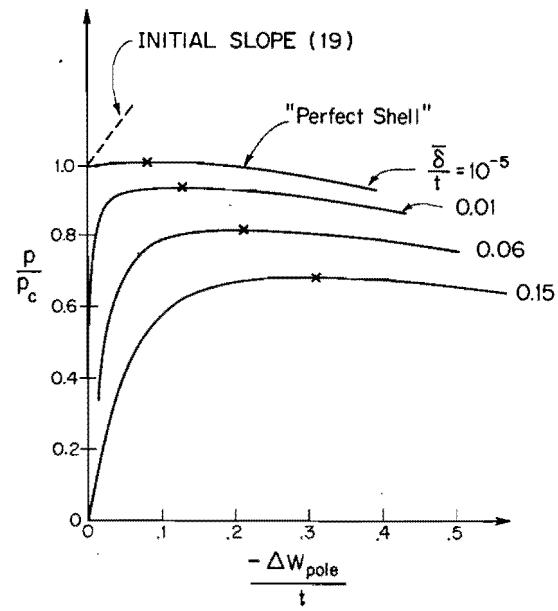

Fig. 6 Curves of pressure versus pole buckling deflection for perfect and imperfect spherical shells (shell parameters are given in the body of the paper)

the tensile stress and strain is used in the examples studied. The form used here is

$$\frac{\epsilon}{\epsilon_y} = \frac{\sigma}{\sigma_y} + \alpha\left(\frac{\sigma}{\sigma_y}\right)^n \tag{37}$$

where σ_y will be referred to as the yield stress in tension and the "yield strain" is defined as $\epsilon_y = \sigma_y/E$. Note that if $\sigma = \sigma_y$, then $\epsilon = (1 + \alpha)\epsilon_y$ so that σ_y is only a reasonable measure of the yield stress if α is small. The tensile curve for $\alpha = 0.1$ and a fairly high hardening rate, $n = 6$, is plotted in Fig. 5, together with the predictions for the critical bifurcation stress, $\sigma_C = -p_C R/(2t)$, as predicted by (21) for J_2 flow theory and (23) for J_2 deformation theory. The ordinate for the bifurcation results (dashed curves) is σ_C/σ_y while the abscissa is $[3(1 - \nu^2)]^{-1/2}t/(\epsilon_y R)$ and with this choice the bifurcation curves fall on the stress-strain curve in the elastic (linear) range. As is typical for plates and shells, the deformation theory predictions fall below those of flow theory.

The example chosen to illustrate the axisymmetric postbuckling behavior is a shell made of material with the stress-strain curve in Fig. 5 and characterized by the additional parameters:

$$[3(1 - \nu^2)]^{-1/2}\frac{t}{\epsilon_y R} = 3, \qquad \frac{R}{t} = 64.5,$$

$$\epsilon_y = 0.00318, \qquad \nu = \tfrac{1}{3} \tag{38}$$

The ratio of the bifurcation pressure to the elastic critical pressur for a shell of the same thickness to radius ratio is 0.492 according to the flow theory formula (21) and 0.455 from the deformation theory result (23). In each case the axisymmetric bifurcation mode is a Legendre polynomial of degree 14.

An imperfection in the form of an axisymmetric initial deflection of the middle surface $\bar{w}$ is taken proportional to the bifurcation mode of the perfect sphere so that

$$\bar{w} = -\bar{\delta}P_{14}(\cos\theta) \tag{39}$$

where $\bar{\delta}$ represents the amplitude of the inward initial deflection at the pole of the sphere. Plots of pressure versus the buckling deflection at the pole are shown in Fig. 6 for various imperfection amplitudes according to the predictions of J_2 flow theory. In this plot, the pressure is normalized by the bifurcation pressure p_C of the perfect shell (21), and ΔW_{pole} is defined to be the difference between the actual deflection at the pole and the deflection of a perfect sphere in the unbifurcated state at the same pressure.

The curve labeled "perfect shell" is really the result of a calculation using an extremely small imperfection, $\bar{\delta} = 10^{-5}t$. The maximum support load is only very slightly above the bifurcation value (21) and it occurs at a buckling deflection of almost one tenth of a thickness as indicated by a cross on the curve. Sketched in Fig. 6 is the lowest possible initial slope of this curve which is consistent with the condition no unloading at bifurcation as predicted by (19). This initial slope for the perfect sphere is rather large; obviously, it can only be a good approximation to the slope in an exceedingly small neighborhood of the bifurcation point. For all practical purposes the maximum support load of the perfect shell, just as in the case of the simple model, is the lowest bifurcation pressure.

Elastic and plastic regions of the shell at two stages of the loading history are given in Fig. 7 along with the middle surface deflection at the corresponding stages for the "perfect" shell just discussed. Prior to the point at which the maximum pressure is attained the elastic zones have grown from nothing (before bifurcation) to the shapes shown at the top of the figure. Once the pressure starts to fall all of the shell but the region near the pole unloads. As shown at the bottom of Fig. 7, the region near the pole dimples inward and continues to deform plastically.

The character of the load-deflection curves for the imperfect spheres in Fig. 6, including the location of the maximum points, is very similar to the analogous curves for the simple model. A plot of the maximum support pressure normalized by $p_0^{\max}$, the maximum support pressure of the perfect shell, as a function of the imperfection amplitude normalized by the shell thickness is given in Fig. 8. The effect of small axisymmetric imperfections on buckling in the plastic range is comparable to their effect in elastic buckling [16, 20–22].

Results based on J_2 deformation theory are also included in Fig. 8, except now $p^{\max}$ is still normalized by the maximum support pressure of the perfect shell as predicted by J_2 flow theory. As just discussed, deformation theory predictions for the perfect shell fall about seven percent below those of flow theory. However, once the imperfection amplitude becomes about one tenth of a shell thickness there is virtually no difference in the buckling

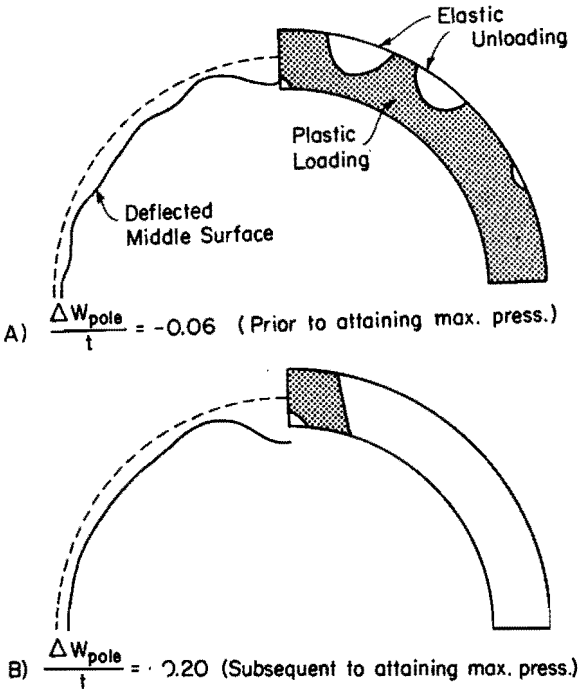

Fig. 7 Current elastic and plastic regions for the perfect spherical shell of Fig. 6 at two points of the deformation history (exaggerated shell thickness and deflection)

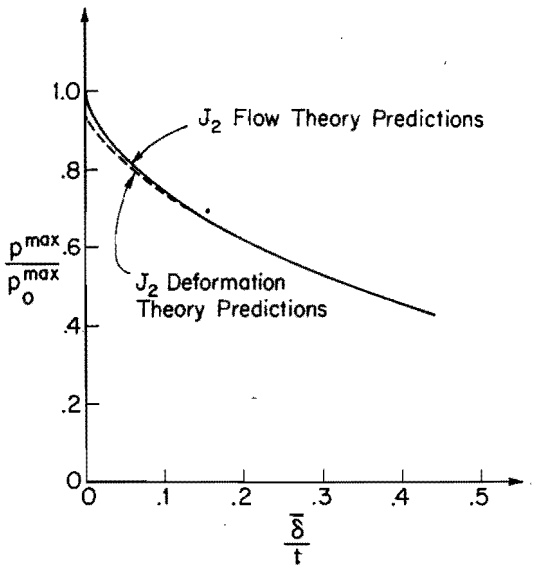

Fig. 8 Buckling pressures for imperfect spherical shells; for both curves p_0^{max} is the maximum support pressure of the perfect shell as predicted by the J_2 flow theory calculation (shell parameters are given in the body of the paper)

pressure predictions. A similar observation was made by Onat and Drucker [28] with respect to the buckling of a cruciform column in compression where the disparity between the bifurcation results of the two plasticity theories was much greater.

The curve of buckling pressure as a function of the imperfection amplitude does not level out at a pressure corresponding to the effective yield pressure of the perfect sphere in the way that the simple model does as discussed in conjunction with Fig. 3. Of course, the shell material in this example has a high hardening rate with a very smooth transition from the elastic to the plastic regime. Instead, the buckling pressure falls steadily with increasing imperfection amplitude and at a value of $\bar{\delta}/t = 0.4$ the buckling load has been reduced by a factor of two.

Some indication of the extent to which the computed buckling pressures are sensitive to the discretization parameters is shown in Table 1. There, N is the number of finite-difference stations from the pole to the equator, M is the number of intervals through the thickness as in (36), I is the number of linear steps in the computation history taken to reach the maximum pressure and the fourth column is the ratio of the computed maximum pressure to the elastic buckling load (14). The numerical values are for the shell of (38) and Fig. 6 with J_2 flow theory and with $\bar{\delta} = 0.15t$. Most of the graphical results were calculated with $N = 50$, $M = 10$ and I between 25 and 30.

We have chosen our second example to illustrate buckling behavior under circumstances in which buckling takes place just outside the elastic range. In practice this might be expected to happen when a structure is inadvertently overloaded or when the yield stress is overestimated. We will also investigate another imperfection shape, the flat spot considered by Budiansky

Table 1

N	M	I	$p^{max}/p_C^{elastic}$
30	6	17	0.338
30	10	17	0.337
50	10	21	0.333
50	10	27	0.331
90	14	27	0.328

[29] and Koga and Hoff [22]. In this case a flat spot of radius $\bar{r}$ and maximum inward deflection $\bar{\delta}$ is located at each pole. The imperfection shape is given by (at the upper pole)

$$\bar{w} = -\bar{\delta}\left\{1 - 3\left(\frac{\theta}{\gamma}\right)^2\left[1 - \left(\frac{\theta}{\gamma}\right)^2 + \frac{1}{3}\left(\frac{\theta}{\gamma}\right)^4\right]\right\}, \quad |\theta| < \gamma$$
$$= 0, \qquad |\theta| > \gamma \tag{40}$$

where $\sin\gamma = \bar{r}/R$. With this choice the slope and the radii of curvatures of the imperfect shell vary continuously across $\theta = \gamma$. A convenient measure of the width of the imperfection is

$$\bar{\lambda} = [12(1 - \nu^2)]^{1/4}\frac{\bar{r}}{\sqrt{Rt}} \tag{41}$$

For elastic buckling, Koga and Hoff [22] found that the critical value of $\bar{\lambda}$ for a given imperfection amplitude was about 4.

In our study, J_2 flow theory is used with the stress-strain relation (37) with $\alpha = 0.1$ and $n = 12$, together with the following shell parameters,

$$[3(1 - \nu)]^{-1/2}\frac{t}{\epsilon_y R} = 1.2, \qquad \frac{R}{t} = 64.5,$$
$$\epsilon_y = 0.00793, \qquad \bar{\lambda} = 4, \qquad \nu = \tfrac{1}{3} \tag{42}$$

For this choice the bifurcation pressure of the perfect shell (21) occurs at 80 percent of the elastic critical pressure (14). As before, the maximum support pressure of the perfect sphere ($\bar{\delta} = 10^{-6}t$) is only very slightly above the bifurcation value p_C. A plot of maximum pressure as a function of the imperfection amplitude is shown in Fig. 9. The results are not unlike those in Fig. 8 for the other imperfection shape (39) except that for very small imperfection amplitudes the bifurcation mode imperfection (39) causes larger relative reductions.

Included in Fig. 9 is a plot of the elastic buckling pressure (i.e., calculated with $\alpha = 0$) in the presence of the same flat spot imperfections. This curve is virtually identical to one given by Koga and Hoff [22] which was obtained by a rather different method of computation for a flat spot at only one pole. Once the buckling pressure has been reduced by about 30 percent, the discrepancy between the elastic predictions and those which account for plastic deformation is very small. Analogous to the

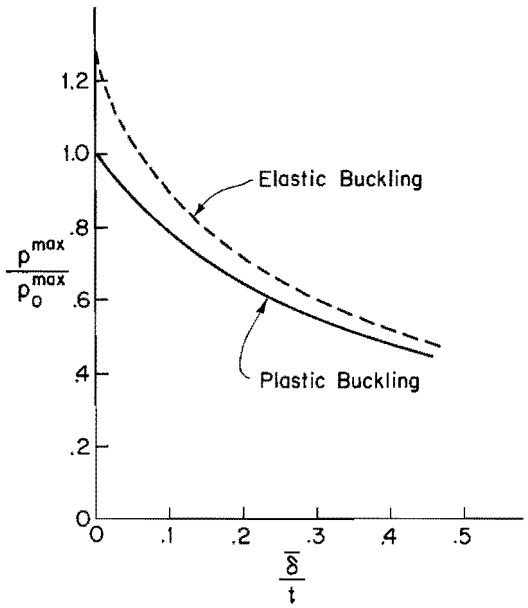

Fig. 9 Buckling pressures for spherical shells with flat spot imperfections, for both curves, p_0^{max} is the maximum support pressure of the perfect shell as predicted by J_2 flow theory (shell parameters are given in the body of the paper)

behavior observed with respect to the simple model, the imperfection reduces the buckling pressure to the point where plastic deformation plays a less important role in the buckling process.

Concluding Remarks

If it is possible to generalize from the two examples investigated here, it would appear that imperfection-sensitivity is potentially as much of a problem for buckling in the plastic range as it is in elastic buckling. In practice, however, it is not likely to cause the large reductions in buckling loads that have to be lived with in some elastic shell structures. This is because, for shell structures made of engineering materials for example, plastic buckling usually requires relatively high thickness to radius ratios and in such circumstances the problem of manufacturing "reasonably perfect" shells is much less difficult than when the thickness-to-radius ratio is very low.

In a series of experiments on hemispherical shells subject to a load applied to the shell through a rigid boss, Leckie [30] found a marked unstable postbuckling behavior in the plastic range. His rigid-plastic analysis of these shells revealed this also. These shells buckled at a limit load and not as a result of anything resembling bifurcation; nevertheless, Leckie's results emphasize that the phenomena investigated here, which are familiar in the elastic buckling, certainly do occur in the plastic range.

Although there are some similarities between the analytic features of bifurcation and buckling in the plastic range and the initial postbuckling behavior of elastic structures, plastic buckling has some distinct characteristics which make an analytic treatment of imperfection-sensitivity very difficult. Not the least of these is the fact that the maximum support load of the perfect structure is not attained at the bifurcation point.

Finally, we mention that we have purposely included predictions based on both of the two popular phenomenological theories of plasticity to emphasize that, for the examples studied here, the predictions are qualitatively the same and our conclusions are not subject to the controversy concerning the use of one of these theories rather than the other.

References

1 Shanley, F. R., "Inelastic Column Theory," *Journal of the Aerospace Sciences*, Vol. 14, 1947, pp. 261–267.

2 Duberg, J. E., and Wilder, T. W., "Inelastic Column Behavior," NACA Report 1072, 1952.

3 Pearson, C. E., "Bifurcation Criterion and Plastic Buckling of Plates and Columns," *Journal of the Aerospace Sciences*, 1950, pp. 417–424.

4 Hill, R., and Sewell, M. J., "A General Theory of Inelastic Column Failure," *Journal of the Mechanics and Physics of Solids*, Vol. 8, 1960, pp. 105–118, and, Vol. 10, 1962, pp. 285–300.

5 Hill, R., "A General Theory of Uniqueness and Stability in Elastic-Plastic Solids," *Journal of the Mechanics and Physics of Solids*, Vol. 6, 1958, pp. 236–249.

6 Hill, R., "Some Basic Principles in the Mechanics of Solids Without a Natural Time," *Journal of the Mechanics and Physics of Solids*, Vol. 7, 1959, pp. 209–225.

7 Koiter, W. T., "Over de Stabiliteit van het Elastisch Evenwicht" ("On the Stability of Elastic Equilibrium"), thesis, Delft, H. J. Paris, Amsterdam, 1945; English translation issued as NASA TT F-10, 1967, p. 833.

8 Koiter, W. T., "Elastic Stability and Postbuckling Behavior," *Proceedings of the Symposium on Nonlinear Problems*, University of Wisconsin Press, Madison, 1963, pp. 257–275.

9 Thompson, J. M. T., "A General Theory for the Equilibrium and Stability of Discrete Conservative Systems," *Zeitschrift für Mathematik und Physik*, Vol. 20, 1969, pp. 797–846.

10 von Karman, Th., Dunn, L. G., and Tsien, H. S., "The Influence of Curvature on the Buckling Characteristics of Structures," *Journal of the Aerospace Sciences*, Vol. 7, 1940, p. 276.

11 Sewell, M. J., "The Static Perturbation Technique in Buckling Problems," *Journal of the Mechanics and Physics of Solids*, Vol. 13, 1965, pp. 247–265.

12 Augusti, G., "Buckling of Inelastic Arches: A Simple Model," *Meccanica*, Vol. 2, 1968, pp. 102–105.

13 Budiansky, B., and Hutchinson, J. W., "Dynamic Buckling of Imperfection-Sensitive Structures," *Proceedings of the Eleventh International Congress of Applied Mechanics*, Munich, Julius Springer-Verlag, Berlin, 1964, pp. 636–651.

14 Mayers, J., and Wesenberg, D. L., "The Maximum Strength of Initially Imperfect Axially Compressed, Circular Cylindrical Shells," Report, Department of Aeronautics and Astronautics, Stanford University, Aug. 1969.

15 van der Neut, A., "De Elastische Stabiliteit van den Dunwandigen Bol" ("The Elastic Stability of the Spherical Shell"), thesis, Delft, H. J. Paris, Amsterdam, 1932.

16 Koiter, W. T., "The Nonlinear Buckling Problem of a Complete Spherical Shell Under Uniform External Pressure," Vols. I, II, III, and IV, *Proceedings, Kon. Ned. Ak. Wet*, Series B, Vol. 72, 1969, pp. 40–123.

17 Bijlaard, P. P., "Theory and Tests on the Plastic Stability of Plates and Shells," *Journal of the Aerospace Sciences*, Vol. 16, 1949, pp. 529–541.

18 Batterman, S. C., "Plastic Stability of Spherical Shells," *Journal of Engineering Mechanics*, ASCE, EM2, 1969, pp. 433–446.

19 Batterman, S. C., "Load-Deformation Behavior of Shells of Revolution," *Journal of Engineering Mechanics*, ASCE EM6, 1964, pp. 1–19.

20 Bushnell, D., "Nonlinear Axisymmetric Behavior of Shells of Revolution," *AIAA Journal*, Vol. 5, 1967, pp. 432–439.

21 Thurston, G. A., and Penning, F. A., "Effect of Axisymmetric Imperfections on the Buckling of Spherical Caps Under Uniform Pressure," *AIAA Journal*, Vol. 4, 1966, pp. 319–327.

22 Koga, T., and Hoff, N. J., "The Axisymmetric Snap-Through Buckling of Thin-Walled Spherical Shells," *International Journal of Solids and Structures*, Vol. 5, 1969, p. 679.

23 Reissner, E., "On Axisymmetrical Deformations of Thin Shells of Revolution," *Proceedings of the Symposium in Applied Mathematics*, Vol. 3, McGraw-Hill, New York, pp. 27–52.

24 Kalnins, A., "Analysis of Shells of Revolution Subject to Symmetrical and Nonsymmetrical Loads," JOURNAL OF APPLIED MECHANICS, Vol. 33, TRANS. ASME, Vol. 88, Series E, 1964, pp. 467–476.

25 Stephens, W. B., and Fulton, R. E., "Axisymmetric Static and Dynamic Buckling of Spherical Caps Due to Centrally Distributed Pressures," *AIAA Journal*, Vol. 7, 1969, pp. 2120–2126.

26 Greenbaum, G. A., and Conroy, D. C., "Postwrinkling Behavior of a Conical Shell of Revolution Subject to Bending Loads," *AIAA Journal*, Vol. 8, 1970, pp. 700–707.

27 Stephens, W. B., "Computer Program for Static and Dynamic Analysis of Symmetrically Loaded Orthotropic Shells of Revolution," NASA TN, D6158, Dec. 1970.

28 Onat, E. T., and Drucker, D. C., "Inelastic Instability and Incremental Theories of Plasticity," *Journal of the Aerospace Sciences*, Vol. 20, 1953, pp. 181–186.

29 Budiansky, B., "Buckling of Clamped Shallow Spherical Shells," *Proceedings of the Symposium on Theory of Thin Elastic Shells*, Delft, 64-94, North Holland Publishing Company, Amsterdam, 1960.

30 Leckie, F. A., "Plastic Instability of a Spherical Shell," *Theory of Thin Shells*, ed., Niordson, F. I., Springer-Verlag, 1969.